Universal Distribution of Residual Carriers in Tetrahedrally Coordinated Amorphous Semiconductors

Baojie Yan, N. A. Schultz, A. L. Efros, and P. C. Taylor
Department of Physics, University of Utah, Salt Lake City, Utah 84112
(Received 2 July 1999)

An uncommon electron spin resonance technique is used to show that a universal distribution of residual carriers exists in tetrahedrally coordinated amorphous semiconductors following optical excitation at low temperatures. This universal behavior at long decay times results because statistical fluctuations in the electron and hole densities cannot occur and therefore do not affect the kinetics. This behavior is confirmed for carrier densities between 10^{16} and 10^{17} cm^{-3} and decay times as long as 10^4 s.

PACS numbers: 72.20.Ee, 71.23.Cq, 72.80.Ng, 76.30.–v

In this Letter we demonstrate that the decay of photoexcited carriers in tetrahedrally coordinated amorphous semiconductors is a universal property of these amorphous solids. In 1989 Shklovskii *et al.* [1] discovered that at low temperatures the simultaneous diffusion and recombination of electron-hole pairs in amorphous semiconductors is a universal property that does not depend on the functional form for the density of localized electronic states. This generally has prompted renewed interest [2] in the diffusion and recombination mechanisms for electrons and holes trapped in localized band-tail states in hydrogenated amorphous silicon (a-Si:H), the quintessential amorphous semiconductor. We report experimental results and theoretical explanations of the generation and recombination kinetics for band-tail electrons and holes in a-Si:H and hydrogenated amorphous germanium (a-Ge:H). The measurements employ an uncommon electron spin resonance (ESR) technique (second harmonic detection or SH-ESR) that surpasses the sensitivity of previous measurements [3,4] by at least 3 orders of magnitude. This increased sensitivity also improves by several orders of magnitude the lower bound on photoexcited carrier concentrations above which nongeminate or distant-pair recombination (recombination where the electron and hole are generated in different quantum transitions) dominates the recombination processes in tetrahedrally coordinated amorphous semiconductors [1,5]. In combination with these measurements, the theory that we develop tests the universality of the diffusion and recombination of photoexcited electrons and holes in amorphous semiconductors at orders of magnitude lower carrier densities and orders of magnitude longer recombination times.

Shklovskii *et al.* [1,5–7] have developed a theory to describe recombination under steady-state conditions. In this Letter, we extend these ideas to describe the recombination kinetics over a wide range of times after cessation of optical excitation. Immediately after the light is switched off the recombination is mainly geminate [the recombining electron and hole were generated in the same optical transition]. The recombination rate is $\tau_r^{-1}\exp(-2R/a)$, where R is the distance between the electron and the hole, a is the effective localization length which for simplicity we assume applies only to the electron, and $\tau_r \approx 10^{-8}$ s. The diffusion time, τ_p, which is controlled by phonons, is $\approx 10^{-12}$ s, and therefore during the early stages of recombination diffusion plays the major role. At low temperatures this diffusion involves only hopping downward in energy for both the electron and the hole, a process that becomes slower and slower in time because of the rapidly decreasing densities of states in the conduction and valence band tails. When the electron and hole are separated by distances greater than $R_c = (a/2)\ln(\tau_r/\tau_p)$, the process is controlled by recombination and diffusion can be neglected. At very large carrier densities, geminate recombination may cease to be important at smaller values of R since this recombination mechanism is less important as soon as R is on the order of the average distance between carriers. In this case most of the carriers survive to times where geminate recombination is unimportant. On the other hand, at very small carrier densities, geminate recombination may continue for $R > R_c$. In this case most of the carriers recombine geminately. However, regardless of the initial carrier densities, at $R \gg R_c$ and $t \gg \tau_r^2/\tau_p = \tau_r \exp(2R_c/a)$ the recombination occurs exclusively between distant pairs.

This problem was originally addressed by Dunstan [8], whose approach was based on a model of randomly distributed electrons and holes. Using a simple mean field equation this model yields an expression for the density of pairs that survive until very long times, which is given by $n(R) = 3/4\pi R^3$ where $R = a\ln(t/\tau_r)/2$. Note that this asymptotic expression is independent of the initial carrier density. However, a computational approach to this problem [9] yields a density $n(R)$ proportional to $R^{-3/2}$ at long times. The latter result is easily interpreted in terms of the Ovchinnikov-Zeldovich effect [10–12], which asserts that, due to statistical fluctuations, at a density n_0 the excess number of carriers of one type in each volume R^3 is on the order of $(n_0R^3)^{1/2}$. These excess carriers cannot recombine within this volume. Therefore, the excess density is $(n_0R^3)^{1/2}/R^3$, which explains the computational results.

 0031-9007/00/84(18)/4180(4)$15.00

On the other hand, electrons and holes are created in pairs, and therefore no pair can be separated more than R_c. Therefore, on a scale $R \gg R_c$ the number of electrons is equal to the number of holes, and *the model of randomly distributed electrons and holes is not relevant to describe large distances and long times.* To eliminate this discrepancy we employ an equation of the same type as that used in Ref. [8], but we impose the condition of charge neutrality. Suppose all pairs with a distance less than R have already recombined, and draw a sphere of radius R around each electron. By definition there will be no holes inside the spheres. Next increase the radii of each sphere from R to $R + dR$, and calculate the average number of holes in these shells. The corresponding decrease of electron density is given by

$$dn_e(R) = -n_e(R)4\pi R^2 n_h(R)dR\,, \tag{1}$$

where n_e and n_h are the densities of electrons and holes, respectively. By charge neutrality $n_e = n_h = n$, and one obtains

$$dn(R) = -n^2(R)4\pi R^2 dR\,. \tag{2}$$

As mentioned above, the recombination at short times is of a different form. To eliminate these processes, we take a solution to Eq. (1) of the form

$$n^{-1} - n_0^{-1} = \frac{4\pi}{3}\,(R^3 - R_0^3)\,, \tag{3}$$

where n_0 and R_0 are a density and a separation at some time when distant pair recombination clearly dominates. At large R one obtains $n(R) \cong [4\pi R^3/3]^{-1}$, which is independent of n_0. This asymptotic expression is not exact; however, recent computer simulations of the problem of particles of one type yields an extra factor of 1.15, which is close to unity [13]. We now compare the growth of the SH-ESR under a wide range of generation rates, G, with the predictions of previous steady-state models [1,5] and the long-time decay of the photoexcited SH-ESR with the predictions of Eq. (3).

In a-Si:H two optically induced electron spin resonance (LESR) signals are commonly observed at temperatures below about 100 K. These two signals, whose characteristic g values are approximately 2.004 and 2.01, are usually attributed to electrons trapped in localized conduction-band-tail states and holes trapped in localized valence-band-tail states, respectively [14]. In addition to these two LESR signals, there is a third, metastable ESR signal centered at $g = 2.0055$ that is attributed to neutral silicon dangling bonds [15]. Because of the small difference in g values, it is often difficult to separate this latter signal from that attributed to band-tail electrons.

Films of nominally undoped a-Si:H were deposited on ESR-grade quartz substrates using a standard plasma-enhanced chemical vapor deposition (PECVD) technique. These films, which were 3 μm thick, had bulk ESR spin densities less than 5×10^{15} cm^{-3}. Five samples were stacked together to perform the LESR experiments. Before measurement, the samples were annealed at 468 K in a dry nitrogen atmosphere for 2 h and then slowly cooled to 300 K. Samples were cooled from 300 to 40 K in the dark. [To obtain maximum sensitivity all data shown in this Letter were taken at 40 K, but the decay curves are independent of temperature from about 5 to 50 K.] ESR and LESR measurements were performed on a Bruker 200D-SRC spectrometer at 9.5 GHz. Variable temperatures, accurate to ± 1 K, were obtained using a Helitran flow system. The excitation source was a He-Ne laser (1.96 eV). Light intensities at the sample were varied from 2×10^{-6} mW/cm^2 to 20 mW/cm^2 using neutral density filters. All spectra were taken with 0.2 mT (2 G) modulation amplitude.

In spite of the limited penetration depth of the exciting light, the LESR signals scaled with sample thickness (the use of two films in a stack reduced the saturated LESR spin density to 40% of the value obtained with five films in the stack). This behavior is presumably due to multiple reflections in the high-Q ESR cavity.

The LESR spectra were obtained using a "rapid passage" technique that employs second harmonic detection (SH-LESR). Because of the long spin-lattice relaxation times (T_1) in a-Si:H at low temperatures ($T_1 \approx 1$ ms at 30 K [2]), this technique provides an effective increase in the sensitivity of detection for the LESR of at least 3 orders of magnitude over the standard first harmonic detection [16]. The results presented in this Letter employ the absorption component [17,18] of the SH-LESR because the dispersion component contains greater noise [19]. The major complication with the SH-LESR technique is that, in addition to the usual ESR parameters, the spin density depends subtly on T_1. For this reason one must carefully compare spectra to known absorption signals to obtain accurate measurements of the spin densities. For this purpose, we have used the standard LESR in a-Si:H at high spin densities.

Since the band-tail hole (broad) and band-tail electron (narrow) lines have slightly different values of T_1 at any given temperature, the exact line shape varies slightly depending on the microwave power employed. These small variations in the effective intensities of the band-tail-electron and band-tail-hole signals with microwave power are not important for the results discussed in this Letter.

The SH-LESR data can be fit accurately by a simple phenomenological model that incorporates bimolecular recombination and dispersion [16]. For generation rates G between 10^{13} and 10^{20} cm^{-3} s^{-1} at approximately 40 K, the value of α is always 0.5 for both growth and decay. Although this fitting clearly identifies the recombination mechanism for the SH-ESR as distant pair and the dispersion as independent of G, there is otherwise no microscopic information to be gained.

The time constants τ as determined by the phenomenological fitting described above, for the growth of the

SH-ESR are shown as a function of G in Fig. 1. From this figure it is clear that τ, which is related to an average recombination lifetime in this phenomenological model, is proportional to $G^{-0.7}$. Levin *et al.* [5] have shown that the dominant radiative recombination process is distant pair (nongeminate) recombination at generation rates G, far below those used in this study (many orders of magnitude below $G = 10^{17}$ cm^{-3} s^{-1}, which corresponds to approximately 10 μW/cm^2 for the thicknesses of samples we have employed). Using computer simulations, these authors have also shown that the mean radiative lifetimes τ are proportional to $G^{-0.84}$ [5], which is in substantial agreement with the results shown in Fig. 1.

Figure 1 also shows the saturated spin densities of band-tail electrons and holes as measured by SH-ESR. The solid triangles are data taken after long time illumination with the light still on. At excitation intensities above about 3×10^{-2} mW/cm^2 the data are consistent with those previously published by Boulitrop and Dunstan [3,20]. Note that at the lowest excitation intensities the data do not reach the saturated values during the time scale of the experiment. [The smaller values were taken after 3.5 h and the larger values after 7 h.] The solid line is a linear regression fit to the solid triangles. The saturated spin densities (with the light on) depend only weakly on the generation rate ($n \propto G^{0.2}$) and are consistent with $G^{0.16}$, as estimated by Levin *et al.* [5] from computer calculations. Because the data of Fig. 1 at the lowest excitation intensities correspond to $G \approx 10^{13}$ cm^{-3} s^{-1}, these results decrease by orders of magnitude the upper bound on G above which the recombination is by distant pairs.

The open triangles in Fig. 1 are the residual SH-ESR spin densities after the light was turned off for 45 min. If the large R approximation to Eq. (3) were strictly applicable after 45 min, then the residual spin densities would be independent of G and therefore exhibit a horizontal line in Fig. 1. Although this trend is approximately correct, there is a finite slope to this line, which we now discuss in more detail.

Figure 2 shows the decay curves when the light has been turned off following saturation of the optically induced SH-ESR signal at various excitation intensities. These decays were taken at the peak of the ESR spectrum, which is predominantly due to the electrons. Similar curves were obtained by monitoring the ESR at a magnetic field where only holes contribute. Also, similar curves were obtained at temperatures between about 20 and 50 K. Finally, experiments on samples with silicon dangling bond defect densities greater by a factor of about 3 also produced similar curves. Although the SH-ESR spin densities of electrons and holes differ by about a factor of 3 and the absolute spin densities are difficult to measure accurately by ESR, these uncertainties do not affect the quality of the fits shown in Fig. 2. The solid lines in Fig. 2 are fits to Eq. (3) with the values of the saturated SH-ESR

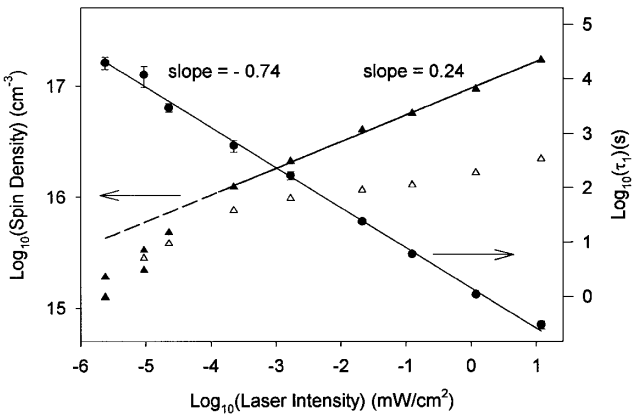

FIG. 1. Right-hand scale: Solid circles represent the characteristic time τ_1 for growth of SH-ESR as a function of light intensity ($\propto G$) in a-Si:H at 40 K [note log-log scale]. Solid line is a linear regression fit to the data. See text for details. Left-hand scale: Spin density of SH-ESR as a function of light intensity in a-Si:H at 40 K. Solid triangles are data after 7 h of illumination time; open triangles are residual data 0.75 h after cessation of illumination. The solid line is a linear regression fit to the solid triangles.

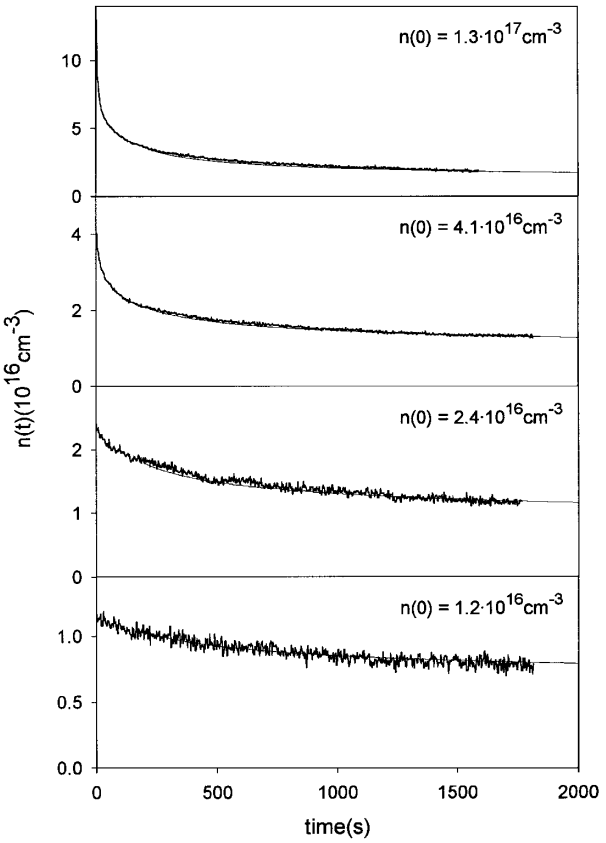

FIG. 2. Decay of SH-ESR in a-Si:H at 40 K after saturation at excitation intensities, from top to bottom, of 19, 2×10^{-1}, 1.6×10^{-3}, and 3.6×10^{-4} mW/cm^2, respectively. Solid lines are theoretical fits to the data using Eq. (3) with $a = 2.4 \times 10^{-7}$ cm. $n(0)$ is the saturated spin density at $t = 0$. See text for details.

spin densities $n(0)$, as given on the figure and an effective localization length of $a = 2.4 \times 10^{-7}$ cm and $\tau_r/\tau_p = 10^4$, which corresponds to $R_0 \approx 3 \times 10^{-6}$ cm in Eq. (3). These fits used $n_0 = n(200\ \text{s})$, but as must be the case, the quality of the fit does not depend on the choice of n_0 for $n_0 \geq 150$ s. Note that we are fitting the absolute intensities $n(t)$ for four excitation intensities, which span about 5 orders of magnitude, with essentially one adjustable parameter—the effective electron localization radius a. Previously reported values of a for a-Si:H vary from about 4 to 10 Å [21–23]. Although our value is larger, there are assumptions associated with any estimate of a, which make comparisons risky.

With the SH-ESR technique we can measure decays such as those shown in Fig. 2 down to saturated carrier densities as low as about 10^{14} cm^{-3}. In addition to being noisier, these decays are very gradual and therefore do not provide a critical test of the theory. However, the decays at low saturated carrier densities are well fit with the same value of a.

To address the question of the universality of Eq. (3) we use as an example a-Ge:H whose optical band gap is approximately half that of a-Si:H and whose exponential densities of localized band-tail states have characteristic energies (inverse slopes) that are at least a factor of 3 greater than a-Si:H. Figure 3 shows a fit for one excitation intensity where the ESR has employed the normal detection technique (derivative of the absorption). In this figure we have used the same value of a as for a-Si:H for simplicity. The decay in a-Ge:H follows the same algebraic form as in a-Si:H even though the two materials have very different densities of localized states at the edges of the bands.

This research was partially supported by NREL under Subcontract No. XAK-8-17619-13 and by NSF under Grant No. DMR-9704946. The authors are indebted to F. C. Marques for permission to use his data for the decay of the optically induced ESR in a-Ge:H. We thank W. D. Ohlsen, D. L. Griscom, W. E. Carlos, and B. I. Shklovskii for helpful discussions.

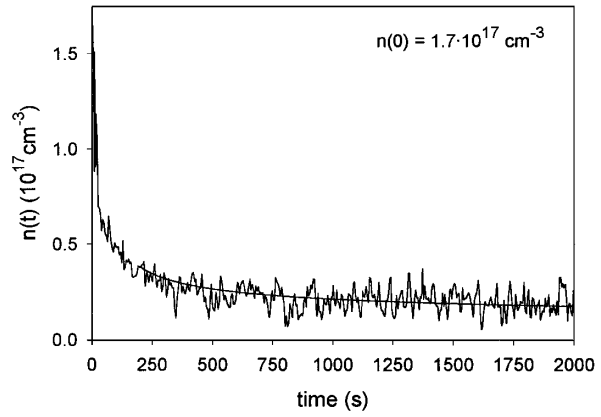

FIG. 3. Decay of ESR (normal first-harmonic detection) in a-Ge:H after saturation at an excitation intensity of approximately 1 W/cm^2. The excitation energy is 1.2 eV. The solid line is a theoretical fit to the data using Eq. (3) and the same parameters as those used in Fig. 2. $n(0)$ is the saturated spin density at $t = 0$.

[1] B. I. Shklovskii, H. Fritzsche, and S. D. Baranovskii, Phys. Rev. Lett. **62**, 2989 (1989).
[2] T. Umeda, S. Yamasaki, J. Isoya, A. Matsuda, and K. Tanaka, Phys. Rev. Lett. **77**, 4600 (1996).
[3] F. Boulitrop and D. J. Dunstan, Solid State Commun. **44**, 841 (1982).
[4] G. Schumm, W. B. Jackson, and R. A. Street, Phys. Rev. B **48**, 14 198 (1993).
[5] E. I. Levin, S. Marianer, and B. I. Shklovskii, Phys. Rev. B **45**, 5906 (1992).
[6] S. D. Baranovskii, E. L. Ivchenko, and B. I. Shklovskii, Sov. Phys. JETP **65**, 1260 (1987).
[7] S. D. Baranovskii, H. Fritzsche, E. I. Levin, I. M. Ruzin, and B. I. Shklovskii, Sov. Phys. JETP **69**, 773 (1989).
[8] D. J. Dunstan, Physica (Amsterdam) **117B & 118B**, 902 (1983).
[9] J. R. Eggert, Phys. Rev. B **29**, 664 (1984).
[10] A. A. Ovchinnikov and Ya. B. Zeldovich, J. Chem. Phys. **28**, 215 (1978); D. Toussaint and F. Wilczek, J. Chem. Phys. **78**, 2642 (1983).
[11] T. M. Searle and J. E. L. Bishop, Philos. Mag. B **53**, L9 (1986).
[12] M. G. Foigel, Sov. Phys. Semicond. **21**, 699 (1987).
[13] L. V. Ponomarev, V. V. Flambaum, and A. L. Efros, Phys. Rev. B **60**, 5485 (1999). In this work, the problem of particles of one type, which can recombine, is studied in connection with a spin problem. The authors find that, at large R, $n(R) = b_d/R^d$ where d is the dimensionality of space. With increasing d, the self-consistent description becomes better [$b_3 = 1.15(3/4\pi)$]. The problem of one type of particles is not strictly equivalent to the present problem, but the results should be close if the neutrality condition is fulfilled on any arbitrarily large scale.
[14] R. A. Street, D. K. Biegelsen, and R. L. Weisfield, Phys. Rev. B **30**, 5861 (1984).
[15] The first attribution of this signal to neutral Si dangling bonds is contained in M. H. Brodsky and R. S. Title, Phys. Rev. Lett. **23**, 581 (1969).
[16] B. Yan and P. C. Taylor, Mater. Res. Soc. Symp. Proc. **507**, 787 (1998).
[17] W. E. Carlos, Jr. (private communication).
[18] W. Weger, Bell Syst. Tech. J. **39**, 1013 (1960).
[19] D. D. Thomas, L. R. Dalton, and J. S. Hyde, J. Chem. Phys. **65**, 3006 (1976).
[20] F. Boulitrop and D. J. Dunstan, J. Non-Cryst. Solids **77 & 78**, 663 (1985).
[21] R. A. Street, *Hydrogenated Amorphous Silicon*, (Cambridge University Press, Cambridge, 1991), p. 298.
[22] C. Tsang and R. A. Street, Phys. Rev. B **19**, 3027 (1979).
[23] M. Stutzmann and J. Stuke, Solid State Commun. **47**, 635 (1983).